Identification of Computational and Experimental Reduced-Order Models

Walter A. Silva *
NASA Langley Research Center
Hampton, Virginia 23681-0001

Moeljo S. Hong †
The Boeing Company
Seattle, Washington 98124-2207

Robert E. Bartels ‡, David J. Piatak §, and Robert C. Scott ¶
NASA Langley Research Center
Hampton, Virginia 23681-0001

The identification of computational and experimental reduced-order models (ROMs) for the analysis of unsteady aerodynamic responses and for efficient aeroelastic analyses is presented. For the identification of a computational aeroelastic ROM, the CFL3Dv6.0 computational fluid dynamics (CFD) code is used. Flutter results for the AGARD 445.6 Wing and for a Rigid Semispan Model (RSM) computed using CFL3Dv6.0 are presented, including discussion of associated computational costs. Modal impulse responses of the unsteady aerodynamic system are computed using the CFL3Dv6.0 code and transformed into state-space form. The unsteady aerodynamic state-space ROM is then combined with a state-space model of the structure to create an aeroelastic simulation using the MATLAB/SIMULINK environment. The MATLAB/SIMULINK ROM is then used to rapidly compute aeroelastic transients, including flutter. The ROM shows excellent agreement with the aeroelastic analyses computed using the CFL3Dv6.0 code directly. For the identification of experimental unsteady pressure ROMs, results are presented for two configurations: the RSM and a Benchmark Supercritical Wing (BSCW). Both models were used to acquire unsteady pressure data due to pitching oscillations on the Oscillating Turntable (OTT) system at the Transonic Dynamics Tunnel (TDT). A deconvolution scheme involving a step input in pitch and the resultant step response in pressure, for several pressure transducers, is used to identify the unsteady pressure impulse responses. The identified impulse responses are then used to predict the pressure response due to pitching oscillations at several frequencies. Comparisons with the experimental data are presented.

Key Words: Aeroelasticity, Unsteady Aerodynamics, Reduced-Order Model

Introduction

At present, the development of CFD-based reduced-order models (ROMs) is an area of active research at several industry, government, and academic institutions.[1] Development of ROMs based on Volterra theory is one of several ROM methods currently under development.[2–7] Reduced-order models based on Volterra theory have been applied successfully to Euler and Navier-Stokes models of nonlinear unsteady aerodynamic and aeroelastic systems. Volterra-based ROMs are focused on the creation of linearized and nonlinear unsteady aerodynamic impulse responses that may then then used in a convolution scheme to provide the linearized and nonlinear responses of the system to arbitrary inputs. In this setting, the linearized and nonlinear impulse responses are the ROMs of the particular nonlinear system under investigation. Upon transformation of the linearized and nonlinear impulse responses into state-space form, the state-space models generated can also be considered ROMs.

Another ROM method, different from the Volterra-based ROM approach, is the Proper Orthogonal Decomposition (POD) technique. The

*Senior Research Scientist, Aeroelasticity Branch, NASA Langley Research Center, Hampton, Virginia;
†Aerospace Engineer, The Boeing Company, Seattle, Washington 98124-2207;
‡Aerospace Engineer, Aeroelasticity Branch, NASA Langley Research Center,Hampton, Virginia;
§Aerospace Engineer, Aeroelasticity Branch, NASA Langley Research Center,Hampton, Virginia;
¶Senior Aerospace Engineer, Aeroelasticity Branch, NASA Langley Research Center,Hampton, Virginia;

POD technique is a method that is used extensively at several research organizations for the development of reduced-order models. A thorough review of POD research activities can be found in Beran and Silva.[1] In addition, a review of the issues involved in the development of reduced-order models for fluid-structure interaction problems is provided by Dowell and Hall.[8] A topic of recent interest is the potential development of hybrid POD/Volterra methods. These hybrid techniques would combine the spatial resolution possible with POD methods with the low dimensionality and computational efficiency of Volterra methods.[9]

The linearization of a nonlinear aeroelastic model is an important first step towards understanding the nature and magnitude of nonlinear aeroelastic phenomena. The response of a linearized system about a nonlinear steady-state condition can be obtained via several methods. Some of these methods include the order reduction of state-space models using various techniques.[10,11] One method for building a linearized, low-order, frequency-domain model from CFD analysis is to apply the exponential (Gaussian) pulse input.[12] This method is used to excite an aeroelastic system, one mode at a time, using a smoothly-varying, small-amplitude Gaussian pulse. The time-domain aeroelastic responses due to the exponential pulse input are transformed into frequency-domain generalized aerodynamic forces (GAFs). These linearized GAFs can then be used in standard linear frequency-domain aeroelastic analyses.[13] Raveh et al[14] applied this method but replaced the exponential pulse input with step and impulse inputs. Raveh[15] also performed parametric variations in order to better understand the numerical issues associated with impulse and step responses, particularly for nonlinear problems. Guendel and Cesnik[16] applied the Aerodynamic Impulse Response (AIR) technique, based on Volterra theory, to the PMARC aerodynamic panel code. The PMARC/AIR code was applied to a simplified High Altitude Long Endurance (HALE) aircraft for rapid linear and nonlinear aeroelastic analysis of the vehicle.

As mentioned above, various inputs can be used in the time domain (using a CFD code) to generate GAFs in the frequency domain in order to perform standard, frequency-domain aeroelastic analyses. But if time-domain aeroservoelastic (ASE) analyses are desired, the frequency-domain GAFs are transformed back into the time domain using traditional rational function approximation (RFA) techniques. These techniques include, for example, the well-known Roger's approximation[17] and the Minimum State technique.[18] The RFA techniques transform frequency-domain GAFs into state-space (time domain) models amenable for use with modern control theory and optimization. The process just described transforms time-domain information (CFD results) into frequency-domain information only to have the frequency-domain information transformed back into the time domain.

Gupta et al[19] and Cowan et al[20,21] applied a set of flight testing inputs to an unsteady CFD code and used the information to create a linear ARMA (autoregressive moving average) model that was transformed into state-space form. Although this technique is applied entirely within the time domain, the shape of the inputs applied to the CFD code requires tailoring in order to excite a specific frequency range, resulting in an iterative process. In a similar vein, Rodrigues[22] developed a state-space model for an airfoil in transonic flow using a transonic small-disturbance algorithm. In the present paper, a direct approach for efficiently generating linearized unsteady aerodynamic state-space models is presented.[23] Although the present application deals with linearized responses based on linearized impulse responses (linearized Volterra kernels), the method can be formally extended to address nonlinear aeroelastic phenomena via the use of nonlinear impulse responses (nonlinear Volterra kernels).

The development of ROMs for computational analyses has proven beneficial to understanding dominant flow physics.[1,23] These ROMs provide insight regarding the level of nonlinearity within a physical process including nonlinear aeroelastic responses and aeroelastic limit cycle oscillations (LCO). Likewise, the development of ROMs for the analysis of experimental data can provide valuable insights regarding the nature of the experimental flow physics and structural response.

Experimental investigation of complex flight dynamic and aeroelastic phenomena are best understood by studying the underlying unsteady aerodynamics. To this end, experiments designed to measure the unsteady aerodynamic response of various configurations provide significant and valuable information.[24–27] Experimental results are compared to various types of numerical analyses (such as CFD) to provide insight into the underlying physics of the problem.

Insight gained from unsteady aerodynamic experiments and analyses can then be used to alter or control some aspect of the underlying physics leading to a modification of the performance of a vehicle. This is the primary goal of the flow control research effort.[28–31] A thorough understanding of the dominant flow physics can lead to an optimal flow control strategy. Therefore, understanding unsteady aerodynamic behavior is an essential step in the design of flow control concepts.

This paper has two purposes: (1) to present the methodology and sample applications of identify-

ing computational reduced-order models for aeroelastic analyses; and (2) to present the methodology and sample applications of identifying experimental reduced-order models for unsteady aerodynamic analyses. As part of the identification of computational ROMs, the paper will discuss the development of linearized, unsteady aerodynamic state-space models for aeroelastic analysis and flutter prediction using the parallelized, aeroelastic capability of the CFL3Dv6 code.[23] As such, this paper begins with a brief description of the CFL3Dv6.0 code. This is followed by an outline of the ROM development process, and a description of the CFD-based impulse response technique. The Eigensystem Realization Algorithm (ERA),[32] which transforms an impulse response into state-space form, is then described. Flutter results for the AGARD 445.6 Aeroelastic Wing and the RSM using the CFL3Dv6.0 code are presented, including computational costs. Unsteady aerodynamic state-space models are then generated and coupled with a structural model within a MATLAB/SIMULINK[33] environment for rapid calculation of aeroelastic responses, including flutter. Aeroelastic responses computed directly using the CFL3Dv6.0 code are compared with the aeroelastic responses computed using the CFD-based ROM within the MATLAB/SIMULINK environment.

As part of the identification of experimental ROMs, the paper demonstrates the feasibility of identifying unsteady aerodynamic impulse responses from experimental unsteady aerodynamic measurements.[34] These experimentally-defined aerodynamic impulse responses can be used to provide insight regarding the dominant flow physics of the experiment. The paper includes a brief description of the methods and experimental facilities used in the identification of these ROMs. Finally, the paper investigates the filtering capability of the deconvolution process that is used to generate the aerodynamic impulse responses.

Description of Computational Methods

The following subsections introduce the parallelized, aeroelastic version of the CFL3Dv6.0 code and an outline of the ROM development process. Two phases of the ROM development process are then described: the identification of unsteady aerodynamic impulse responses and the transformation of these impulse responses into state-space form.

CFL3Dv6.0 Code

The aeroelastic computational fluid dynamics code used in this study is CFL3Dv6.0 code, which solves the three-dimensional, thin-layer, Reynolds averaged Navier-Stokes equations with an upwind finite volume formulation.[35,36] The code uses third-order upwind-biased spatial differencing for the inviscid terms with flux limiting in the presence of shocks. Either flux-difference splitting or flux-vector splitting is available. The flux-difference splitting method of Roe[37] is employed in the present computations to obtain fluxes at cell faces. There are two types of time discretization available in the code. The first-order backward time differencing is used for steady calculations while the second-order backward time differencing with subiterations is used for static and dynamic aeroelastic calculations. Furthermore, grid sequencing for steady state and multigrid and local pseudo-time stepping for time marching solutions are employed. In this paper, multiblock MPI parallel aeroelastic computations, including flutter, are performed.

ROM Development Process

An outline of the ROM development process is as follows:

1. Implementation of impulse response technique into aeroelastic CFD code;

2. Computation of impulse responses for each mode of an aeroelastic system using the aeroelastic CFD code;

3. Impulse responses generated in Step 2 are input into the ERA code;

4. Evaluation/validation of the state-space models generated in Step 3;

Steps 1 and 2 are described in greater detail in the references that address Volterra-based Reduced-Order Models (ROMs) such as Refs. 3-7. The basic premise of Volterra-based ROMs is the extraction of linear and nonlinear kernel functions that capture the input-output functional relationship between, for example, unsteady motion of a wing (input) and the resultant loads created by that motion (output). For Volterra-based ROMs, these kernel functions are linearized/nonlinear impulse response functions. A brief overview of Steps 2 and 3 is presented in the following sections.[23]

CFD-Based Discrete Unit Impulse Response Technique

An aeroelastic system can be viewed as the coupling of an unsteady aerodynamic system (flow solver) with a structural system. The majority of computational aeroelastic methods can be represented by the coupling of the flow solver (nonlinear aerodynamic system) with a linear structural model (Figure 1). The present study focuses on the development of an unsteady aerodynamic ROM (Figure 2) that is then coupled to a structural model for aeroelastic analyses.

A standard technique for computing linearized generalized aerodynamic forces (GAFs) for an aeroelastic system with n modes using a CFD code is the application of a Greens function (influence function) approach. Using the CFD code, each

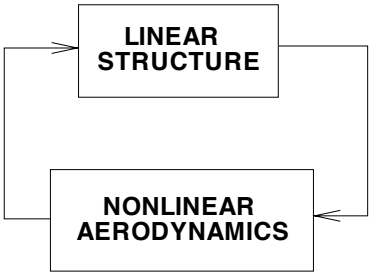

Fig. 1 Coupling of structure and aerodynamics within an aeroelastic CFD code.

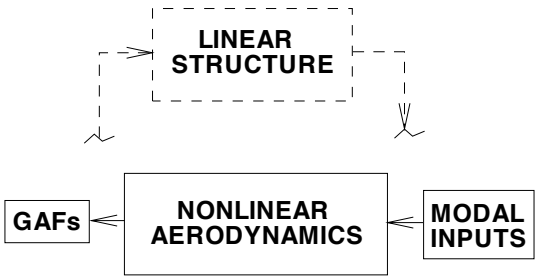

Fig. 2 Identification of generalized aerodynamic forces (GAFs).

structural mode is individually excited to obtain the response of all the modes to this excitation. This process is applied to all n modes, resulting in an n by n "matrix" of responses. The term "matrix" is in quotes to indicate that the responses obtained using this method are usually time-domain functions rather than constants that usually populate a standard matrix.

This technique is a linearization by virtue of the fact that, in a computational aeroelastic analysis, the input to the nonlinear flow solver is the total physical deformation of the wing consisting of the weighted summed total of all the modal responses of interest. By applying a separate excitation to each mode through the nonlinear flow solver, the total nonlinear aeroelastic response is being approximated by a linear superposition of its individual responses. For a linear flow solver, this approach would be exact. This approximation is valid only for small input amplitudes. This is not necessarily a drawback as, quite often, the linearized dynamic aeroelastic response about a nonlinear steady (or static aeroelastic) condition is a reasonable representation of the nonlinear aeroelastic system under investigation. Although not presented in this paper, methods have recently been developed that will enable simultaneous excitation of all the modes.

There are three types of modal excitation inputs that are typically used when implementing this technique. The first is a brute-force approach based on the input of sine waves of individual frequencies. The individual modal responses to these inputs for n modes and r frequencies requires n times r separate code evaluations. In addition, the time length required for each one of these evaluations can be quite large (i.e., computationally expensive) in order to get an adequate number of cycles for adequate frequency resolution, especially for the lower frequencies. This approach is clearly the least efficient.

A second, more elegant approach, involves the use of an exponential (Gaussian) pulse.[12] The exponential pulse can be shaped to excite a particular range of frequencies. Because an exponential pulse excites a pre-selected frequency range, only one code evaluation is required per mode. This is a significant computational savings compared to the brute-force approach, but shape optimization of the exponential pulse may be required when targeting a particular frequency range. In addition, the exponential pulse appears to be strictly limited to linearized analyses. Whereas the impulse function finds formal application to nonlinear problems via Volterra theory, the inclusion of the exponential pulse within a Volterra-type theoretical framework is undefined.

A third, recently-developed, approach consists of replacing the exponential pulse input with a unit impulse.[3–6] The unit impulse excites the entire frequency range of a system so that shape optimization to excite a particular range of frequencies is not necessary. In addition, due to the simplicity of the input and the short amount of time required for convergence, each solution is computed with significant computational efficiency.

System/Observer/Controller Identification Toolbox (SOCIT)

In structural dynamics, the realization of discrete-time state-space models that describe the modal dynamics of a structure has been enabled by the development of algorithms such as the Eigensystem Realization Algorithm (ERA)[32] and the Observer Kalman Identification (OKID)[38] Algorithm. These algorithms perform state-space realizations by using the Markov parameters (discrete-time impulse responses) of the systems of interest. These algorithms have been

combined into one package known as the System/Observer/Controller Identification Toolbox (SOCIT)[39] developed at NASA Langley Research Center.

The primary algorithm within the SOCIT group of algorithms used for the present system realization is the ERA. A brief summary of the basis of this algorithm follows.

A finite dimensional, discrete-time, linear, time-invariant dynamical system has the state-variable equations

$$x(k+1) = Ax(k) + Bu(k) \tag{1}$$

$$y(k) = Cx(k) + Du(k) \tag{2}$$

where x is an n-dimensional state vector, u an m-dimensional control input vector, and y a p-dimensional output or measurement vector with k being the discrete time index. The transition matrix, A, characterizes the dynamics of the system. The goal of system realization is to generate constant matrices (A, B, C, and D) such that the output responses of a given system due to a particular set of inputs is reproduced by the discrete-time state-space system described above.

For the system of Eqs. (1) and (2), the time-domain values of the discrete-time impulse response are also known as the Markov parameters and are defined as

$$Y(k) = CA^{k-1}B \tag{3}$$

with B an (n x m) matrix and C a (p x n) matrix. The ERA algorithm begins by defining the generalized Hankel matrix consisting of the discrete-time impulse responses for all input/output combinations. The algorithm then uses the singular value decomposition (SVD) to compute the A, B, and C matrices.

In this fashion, the ERA is applied to unsteady aerodynamic impulse responses to construct unsteady aerodynamic state-space models.

Description of Experimental Facilities, Models, and Methods

Transonic Dynamics Tunnel (TDT)

The Langley Transonic Dynamics Tunnel (TDT) is a unique national facility dedicated to identifying, understanding, and solving relevant aeroelastic problems. The TDT is a closed-circuit, continuous-flow, variable-pressure, wind tunnel with a 16-foot square test section with cropped corners. The tunnel uses either air or a heavy gas as the test medium and can operate at stagnation pressures from near vacuum to atmospheric, has a Mach number range from near zero to 1.2 and is capable of maximum Reynolds numbers of about 3 million per foot in air and 10 million per foot in heavy gas. The current TDT heavy gas test medium is 1,1,1,2 tetrafluoroethane, R-134a.[40,41] The TDT is specially configured for flutter testing, with excellent model visibility from the control room and a rapid tunnel shutdown capability for model safety (bypass valves). Model mount systems include a sidewall turntable for semispan models, a variety of stings for full-span models, an Oscillating Turntable (OTT), and a cable-mount system for "flying" models.

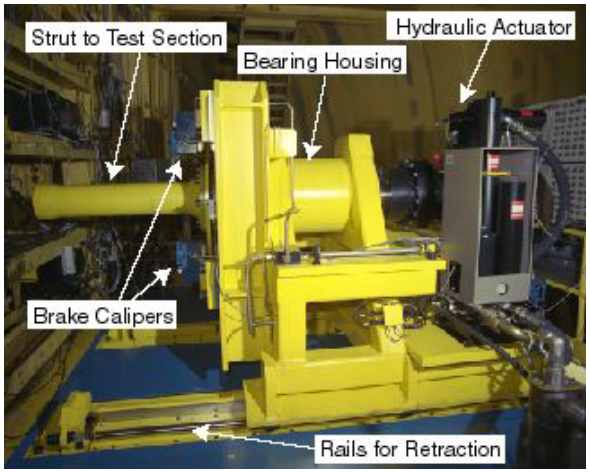

Fig. 3 Side view of the Oscillating Turntable (OTT).

Oscillating Turntable (OTT)

The OTT is a unique research tool at the TDT that provides the ability to oscillate relatively large, semispan wind-tunnel models in pitch at frequencies up to 40 Hz. This research tool has been designed specifically for the acquisition of unsteady pressure and loads data on rigid wind-tunnel models in order to study flow phenomena associated with flutter, LCO, shock dynamics, and nonlinear unsteady aerodynamic effects on a wide variety of aerospace vehicle configurations at transonic speeds. It is anticipated that unsteady pressure measurements due to precisely controlled model motions will provide valuable data for CFD correlation and aircraft design with respect to unsteady aerodynamic/aeroelastic phenomena.[25] Models may be oscillated sinusoidally at constant or varying frequencies, be subjected to a step input, or undergo user-defined motions.

Figure 3 highlights key components of the OTT. The OTT utilizes a powerful rotary hydraulic actuator, rated at 495,000 in-lbf, and a digital Proportional, Integral, Derivative, Feedforward (PIDF) control system to position and oscillate models. Power for the OTT is supplied by a 3000 psi, 150 gpm hydraulic power unit which is located outside the tunnel pressure shell.

Rigid Semispan Model (RSM)

The RSM planform is a 1/12th scale configuration based on an early design known as the Ref-

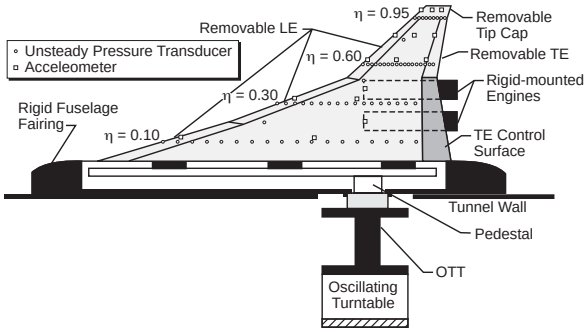

Fig. 4 Planform, model details, and instrumentation layout for the RSM wind-tunnel model.

erence H configuration that was a component of the High Speed Research (HSR) program. Model airfoil shapes were based on those of the Reference H, with the model wing thickness being increased to a constant 4% thickness-to-chord ratio in order to accommodate pressure instrumentation at the wing tip. The model was designed to be very stiff to allow the measurement of aerodynamic properties with only negligible effects of structural deformations.

Figure 4 shows the planform layout and main components of the RSM including the OTT mount. The leading and trailing edges were removable in order to access pressure instrumentation in those regions. A removable tip cap allowed access to pressure instrumentation at the wing tip. The RSM could be tested either with or without a pair of flow-through nacelles. The nacelles were rigidly attached to pylons on the lower, inboard surface of the wing. The RSM wing had a graphite epoxy composite structure with an open-cell foam core.

The instrumentation layout for the RSM (visible in Figure 4) consisted of 131 insitu unsteady pressure transducers located at the 10, 30, 60, and 95% span stations. Six additional unsteady pressure transducers were installed at the 20% chord station for the 20, 45, and 75% span stations for both upper and lower surfaces. Channels were carved into the foam core to accommodate the wiring for the instrumentation. Instrumentation also included accelerometers installed throughout the wing. The fuselage fairing used for testing the RSM on the OTT was instrumented with unsteady pressure transducers. For the flutter analysis using the RSM,[7] the first four structural modes were softened in order to create a flutter response. The purpose of this model was to compare full CFD aeroelastic analyses with ROM aeroelastic analyses and to use the data acquired with the RSM on the OTT for identification of experimental ROMs.

Benchmark Supercritical Wing (BSCW)

The BSCW is shown mounted in the TDT test section in Figure 5. The model has a rectangu-

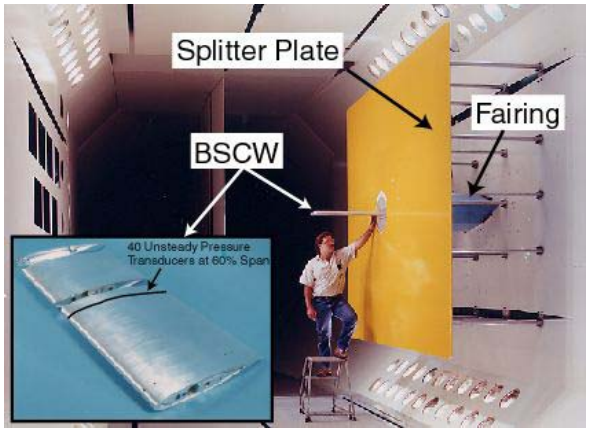

Fig. 5 The Benchmark Supercritical Wing wind-tunnel model.

lar planform with a 32 inch span, 16 inch chord, and a NASA SC(2)-0414 airfoil. Using 40 in-situ transducers, unsteady pressure measurements were made along the chord at the 60 percent spanwise location at Mach numbers ranging from 0.4 to 0.85 and dynamic pressures of 100, 170, and 200 psf in R-134a heavy gas. Reynolds numbers based on model chord ranged from 2.4 to 6.5 million and these test conditions corresponded to reduced frequencies (k) from 0.011 to 0.579 for the BSCW (1 Hz to 30 Hz). Boundary-layer transition was fixed at 7.5 percent chord and the OTT pitch axis was located at x/c=0.3. The BSCW model has been previously tested at the TDT as part of the Benchmark Models Program[42,43] during which a large database of unsteady pressures were obtained during motions on a flexible pitch and plunge mount. The purpose of this model was to use the data acquired using the OTT for the identification of experimental ROMs.

Experimental Methodology

Unsteady pressure measurements were made on the RSM and the BSCW while the models underwent pitch oscillations on the OTT at frequencies from 1 to 10 Hz (RSM) and from 1 to 30 Hz (BSCW). In addition, unsteady pressures were acquired during RSM/OTT and BSCW/OTT step inputs in order to provide data to compute aerodynamic impulse responses.

The identification of experimental unsteady aerodynamic (pressure) ROMs can be performed by using the same techniques used to identify the computational unsteady aerodynamic ROMs. The Volterra theory of nonlinear systems is used as the basis for modeling the linear and nonlinear dynamic response of the unsteady aerodynamic system under investigation, as described in the references.

For the present study, the identification of experimental unsteady aerodynamic impulse responses will be limited to the first-order, or linearized,

kernel. It is referred to as a linearized kernel since identification of the kernel (impulse response) may occur about a nonlinear steady-state condition (such as a transonic Mach number). Future research will focus on the identification of the second-order kernel. The frequency-domain version of the second-order kernel is known as the bi-spectra, which has found important applications across a wide variety of disciplines for quantifying experimental nonlinear dynamics.[44]

The identification of the experimental unsteady aerodynamic impulse responses (first-order kernel) will consist of the deconvolution of a given input/output pair. Deconvolution involves the extraction of the impulse response of a system when the input and corresponding output are known. The input, in this case, is a sequence of positive and negative step inputs in pitch applied using the OTT and the output is any of several measured pressure responses from the wind-tunnel models. Deconvolution is then used to extract the impulse response for the given input/output pair. For the given OTT step input, an impulse response can be identified for each pressure measurement (sensor) on the wind-tunnel models.

Once the impulse response has been generated, convolution is used to predict the pressure response due to sinusoidal inputs in pitch at various frequencies.[34] The measured results are compared to the predicted results (via convolution) in a subsequent section.

Computational Results

The AGARD 445.6 Aeroelastic Wing has been used extensively by several authors to validate computational methods.[13,19,45] Although the aeroelastic behavior of this wing is fairly benign, the aeroelastic data from the flutter test of this wing has been used significantly in the past for the validation of computational techniques.[46] The wing is a 45-degree swept-back wing with a NACA 65A004 airfoil section, panel aspect ratio of 1.65, and a taper ratio of 0.6576. The shapes of the first four structural modes for this wing are presented in Figure 6. The modes are first bending, first torsion, second bending and second torsion. The corresponding modal frequencies in vacuo are 9.60, 38.2, 48.35, and 91.54 Hz. Additional details regarding this wing can be found in the references.

AGARD 445.6 Wing

Full CFD Flutter Solution

This section presents results based on the traditional full CFD flutter solution. The flutter solution is obtained by iterating between the nonlinear aerodynamic system (flow solver) and the structural system at a given Mach number and dynamic pressure entirely within the CFD code. The output of this solution consists of a time history

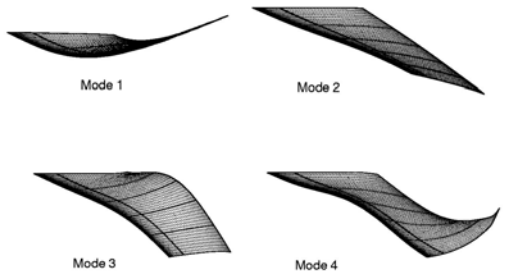

Fig. 6 Structural modes for the AGARD 445.6 Wing.

of the generalized coordinates of the aeroelastic system. Depending on the nature of this aeroelastic response (divergent or convergent), a new dynamic pressure is selected and a corresponding flutter solution is computed. This iterative process is used to define the flutter boundary at several Mach numbers. The results presented in this paper are for the solution of the Euler equations within CFL3Dv6.0.

Figure 7 presents the response of each of the four generalized coordinates at a Mach number of 0.9, a dynamic pressure of 89.3 psf, and a structural damping value (g) of zero. The divergent nature of the first and second modes indicates that this condition is above the flutter boundary. By performing similar analyses at different dynamic pressures, a dynamic pressure of 75 psf was determined to be the flutter dynamic pressure (neutral stability point) for this Mach number. The corresponding flutter frequency was 14.8 Hz. The aeroelastic response at a dynamic pressure of 75 psf is presented as Figure 8, indicating a condition very close to the neutral stability of the aeroelastic system at this condition. These solutions were computed using a non-dimensional time step of 0.3 with 5 subiterations per time step and use of multigrid capability for error reduction and convergence acceleration. Results from the full CFD flutter analysis[23] are consistent with those from Lee-Rausch[13] and other Euler flutter results.[19]

The computational cost for one flutter solution (at a given Mach number and dynamic pressure) is 71 CPU hours for the number of cycles shown in Figures 7 and 8. This is the total CPU cost but, using 96 processors, the actual execution time is approximately 45 minutes on an Origin 2000 cluster. The total time elapsed from the moment the job is submitted for execution, however, can vary depending on the number of other jobs (from different users) in the queue for the computer re-

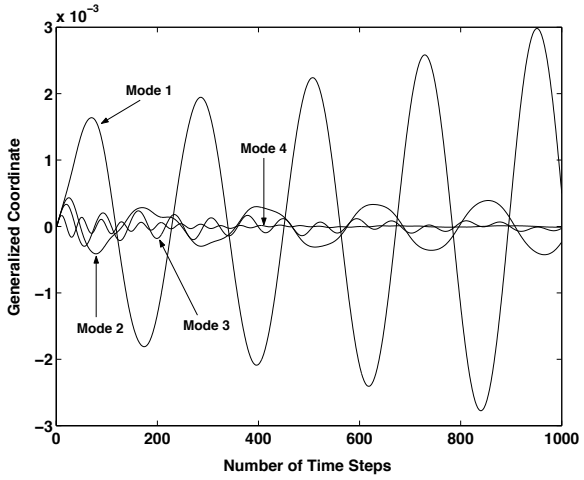

Fig. 7 Aeroelastic transients in terms of generalized coordinates at M=0.9 and q=89.3 psf for AGARD 445.6 Wing.

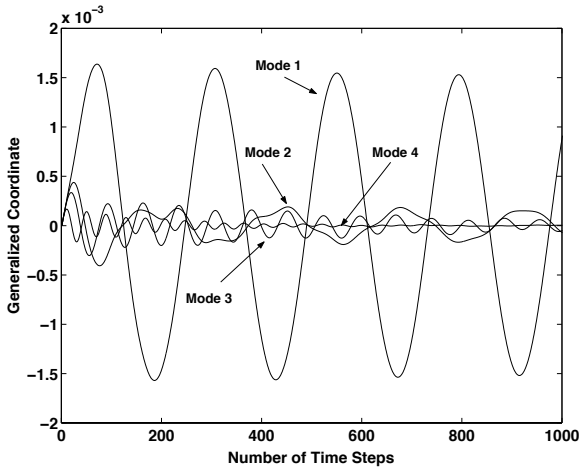

Fig. 8 Aeroelastic transients in terms of generalized coordinates at M=0.9 and Q=75.0 psf for AGARD 445.6 Wing.

sources. The total elapsed time for a single flutter solution can therefore range from 45 minutes to several hours if the job queue is busy. In addition, although four cycles of the lowest frequency mode appear to be sufficient for visually determining the stability of the system, accurate computation of the relevant aeroelastic frequency and damping requires additional cycles. If the number of cycles is doubled to eight cycles, the computational costs increase proportionately to 142 CPU hours and 90 minutes of execution time. The total time elapsed can range from 90 minutes to several hours depending on the number of jobs in the queue.

These costs are, of course, a function of the aeroelastic properties of the system under investigation. The use of parallel processing clearly provides significant improvement in computational time. However, the computational costs (CPU) are still high because parallelization, obviously, does not reduce the amount of computation that needs to be done. Nonetheless, this is a significant improvement over computations performed on a serial platform.

Assuming four dynamic pressure solutions per Mach number, the cost of computing a flutter point (at one Mach number) is 568 CPU hours, requiring at least 360 minutes of execution time. The actual time invested, however, can be on the order of days since the value of dynamic pressure selected for the subsequent analysis depends on the results obtained from the previous analysis. If additional analyses involving parametric variations of structural parameters (damping and frequencies) are needed, additional flutter solutions would be required, increasing computational costs (CPU and time). Finally, as can be seen, the output of traditional CFD-based flutter analyses are aeroelastic transients which provide frequency and damping information at a given flight condition. These transients can certainly be used to define the flutter boundary of the aeroelastic system under investigation but do not comprise a mathematical model of the system itself. In order to develop a mathematical model of the system itself, a ROM is needed.

ROM Flutter Solution

Coupling the state-space model of the unsteady aerodynamic system with a state-space model of the structure within MATLAB/SIMULINK results in a state-space aeroelastic system. The aeroelastic response of the system is a function of the initial conditions of the structure and the dynamic pressure.

In order to validate this state-space aeroelastic system, simulations were performed at various dynamic pressures. Figure ?? presents the generalized coordinate time histories and the corresponding generalized coordinate FFTs at zero dynamic pressure (wind-off). The zero dynamic pressure eliminates all aerodynamic effects, leaving only structural effects. With zero structural damping, the response consists of, in the time domain, the simple harmonic motion of the uncoupled vibration modes and, in the frequency domain, frequency peaks of the uncoupled vibration modes: 9.60, 38.2, 48.35, and 91.54 Hz.

At a dynamic pressure of 75 psf, Figure ??, flutter is evident. The corresponding flutter frequency of 14.5 Hz is clearly identified in Figure ??. A close-up of this aeroelastic transient is presented as Figure 11. This result shows excellent comparison with the result of Figure 8, which was computed using CFL3Dv6.0 directly. In fact, the ROM results showed excellent comparison with results using CFL3Dv6.0 directly at all dynamic pressures investigated.

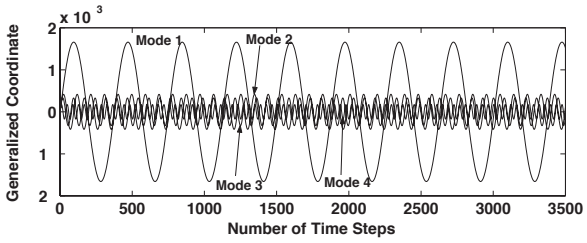

a) Time domain

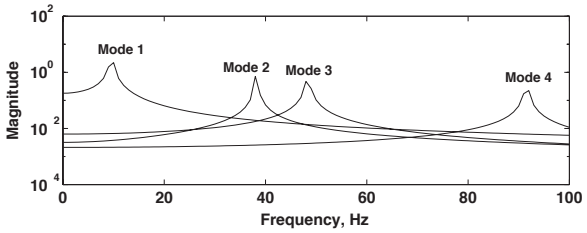

b) Frequency domain

Fig. 9 Aeroelastic response of the reduced-order aeroelastic model at M=0.9 and q=0 psf for AGARD 445.6 Wing.

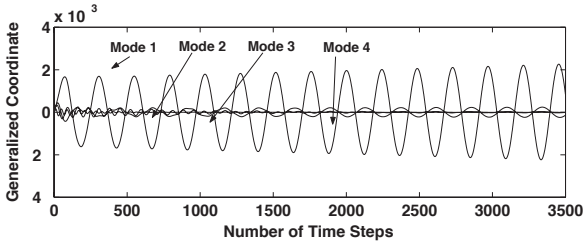

a) Time domain

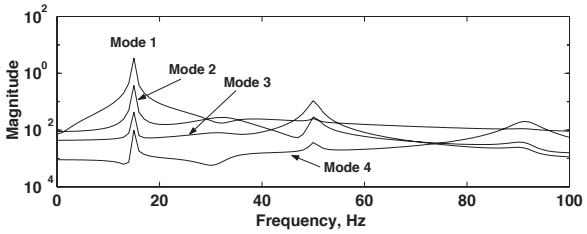

b) Frequency domain

Fig. 10 Aeroelastic transients in terms of generalized coordinates for the reduced-order model at M=0.9, q=75 psf, and g=0.0 for AGARD 445.6 Wing.

These aeroelastic transients are computed in seconds within MATLAB/SIMULINK, thus allowing a larger number of cycles to be computed for improved frequency resolution. In addition, if parametric variations that involve the structure are desired (structural damping, updated frequencies, etc), the analyses can be performed since the unsteady aerodynamic system is unaffected by these variations.

These results validate the ROM methodology presented and are examples of a new and powerful tool available to the aeroelastician. Most importantly, the state-space models developed are

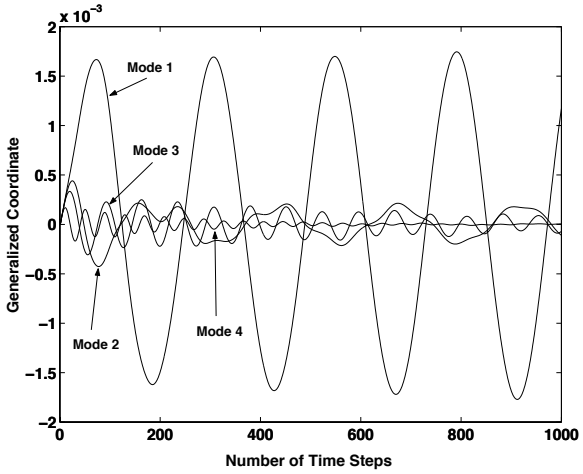

Fig. 11 Close-up of the aeroelastic transients for the reduced-order model at M=0.9, q=75 psf, and g=0.0 for AGARD 445.6 Wing.

suitable for use within a mutidisciplinary design environment, including ASE analysis and design.

Rigid Semispan Model

Results comparing fully coupled aeroelastic solutions to ROM aeroelastic solutions using the softened version of the RSM[7] are presented Figure 12, Figure 13, and Figure 14. Even though some differences in the responses is apparent, the ROM aeroelastic solutions are in excellent agreement with the fully coupled aeroelastic solutions. Both methods predict the neutral stability condition (flutter) at approximately 123.8 psf.

Each fully coupled CFL3Dv6.0 computation required approximately 108 CPU hours on an Origin-3000 computer. Each impulse response (subsequently used to develop aeroelastic ROM) required approximately 312 hours. The computational cost of the impulse responses could have been reduced by optimizing time step, subiterations, and other parameters. It is important to note, however, that each impulse response computation provides the wide range of reduced frequencies as well as the entire range of dynamic pressures. On the other hand, each fully coupled calculation only provides a single dynamic pressure. Research is currently focused on the simultaneous excitation of multiple modes in order to reduce the number of impulse responses required (currently one per mode) to generate the aeroelastic ROM.

Experimental Results

Rigid Semispan Model

Results for the RSM/OTT are presented in this section. The RSM has a total of 131 in-situ pressure transducers. A step input in pitch using the OTT results in 131 unsteady pressure responses. Therefore, deconvolution can be applied to all of the unsteady pressure measurements to yield 131

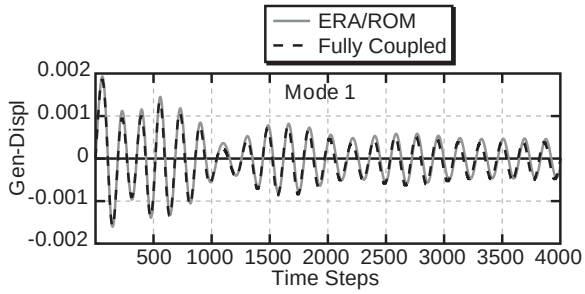

a) Mode 1

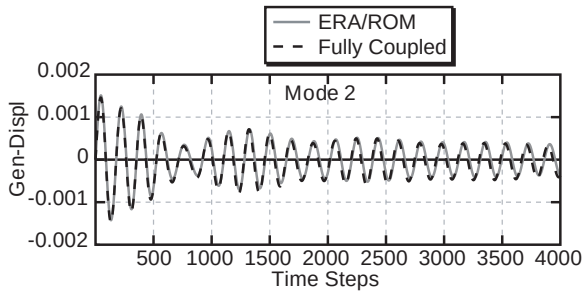

b) Mode 2

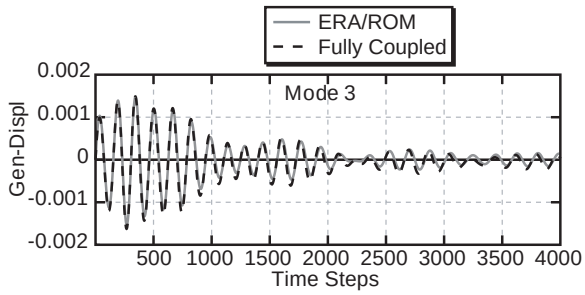

c) Mode 3

Fig. 12 Fully coupled versus ROM aeroelastic solutions for the softened RSM at M=0.7, q=118.08 psf.

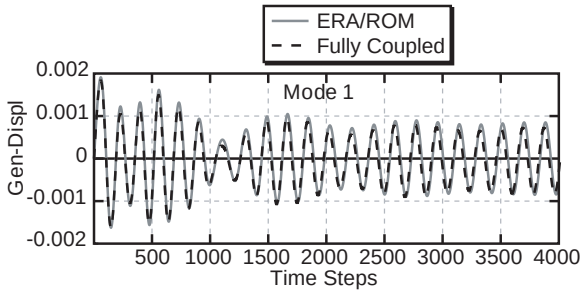

a) Mode 1

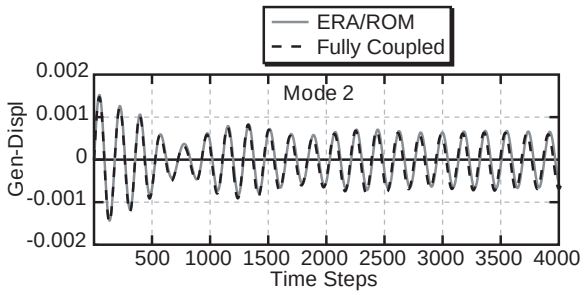

b) Mode 2

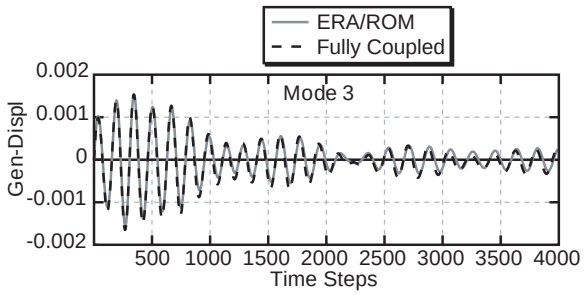

c) Mode 3

Fig. 13 Fully coupled versus ROM aeroelastic solution for the softened RSM at M=0.7, q=123.84 psf.

unsteady aerodynamic impulse responses. For the sake of brevity and to demonstrate the feasibility of the method, results are presented for only one pressure measurement located on the upper surface of the RSM at the 60% span location and the 30% chord station. The data was acquired at a Mach number (M) of 0.8, a dynamic pressure (q) of 150 psf, and with the RSM at zero degrees angle of attack.

Figure 15 presents the step pitch input commanded to the OTT and the resultant pressure response at the pressure transducer location mentioned above. Although a theoretical step input consists of an infinite slope where the step occurs, a physically realizable step input, such as that commanded by the OTT, will be limited by the pitch inertia, stress, and load limitations of the model undergoing pitch. As can be seen, a step input that closely approaches a theoretical step input can, in fact, be applied by the OTT. The unsteady pressure measurement is also quite noisy, as can be seen.

Using the sequence of step pitch motions of the OTT as the input and the unsteady pressure measurement as the output, deconvolution is applied to identify the unsteady aerodynamic impulse response. Figure 16 presents the time- and frequency-domain versions of the pressure impulse response identified via deconvolution. As can be seen in Figure 16(b), the identified impulse response exhibits significant frequency content, as is to be expected for an impulse response. An analysis of the unsteady aerodynamic impulse responses at all pressure transducer locations can provide a spatial mapping of the frequency characteristics of a given configuration at a given test condition. This type of spatial mapping may be useful for the design and optimal placement of various flow control devices.

Upon identification, the unsteady aerodynamic impulse response can then be used to predict the unsteady aerodynamic response due to any OTT

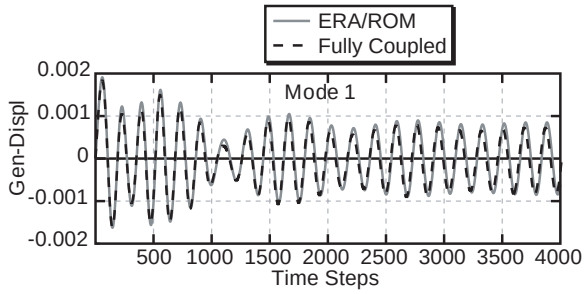

a) Mode 1

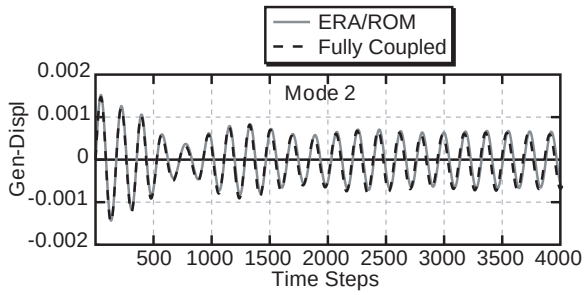

b) Mode 2

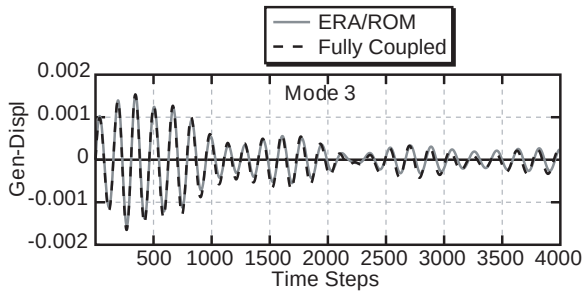

c) Mode 3

Fig. 14 Fully coupled versus ROM aeroelastic solution for the softened RSM at M=0.7, q=129.60 psf.

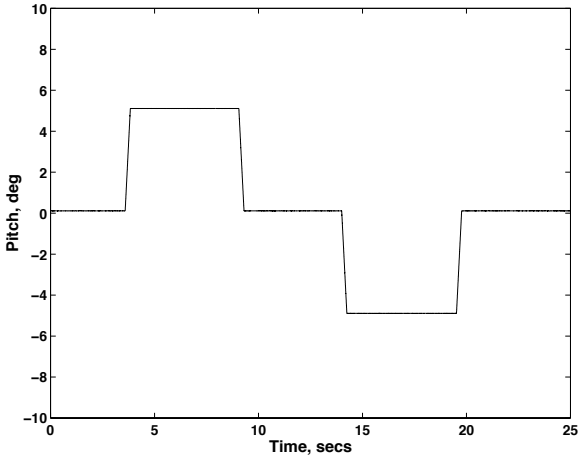

a) Step Input in Pitch

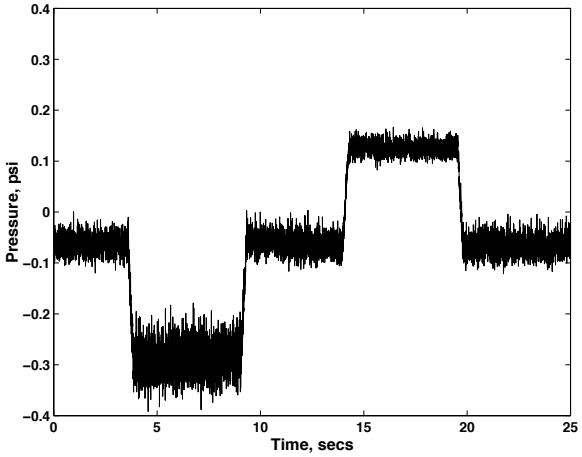

b) Pressure Response due to Step Input in Pitch

Fig. 15 Commanded pitch motion and resultant pressure response on the upper surface of the RSM at 60% span and 30% chord at M=0.8, q=150 psf.

input using convolution and the impulse response of Figure 16. In the following figures, comparisons are made between predicted unsteady aerodynamic responses and the measured responses for several sinusoidal OTT motions.

Figure 17 presents the comparison between the measured pressure response and the corresponding predicted pressure response for a commanded oscillation of 1.2 Hz. The comparison is excellent and demonstrates the ability of the method to capture the dominant (driving) frequency while filtering out uncorrelated noise. The process of identifying the correlation for a given input/output pair, via deconvolution, has the added benefit that it filters out any information that is not correlated to the input/output correlated. Therefore, uncorrelated measurement noise, for example, is automatically removed as the impulse response is generated. This filtering capability is visible in Figure 17(b).

Figure 18 presents the comparison between the measured pressure response and the corresponding predicted pressure response for a commanded oscillation of 10.1 Hz. For this case, without the predicted response, it would be very difficult to discern any periodicity in the measured response. The filtering capability of the deconvolution method proves to be essential at this frequency.

At this condition, M=0.8 and q=150 psf, the linearity of the measured pressure responses (for this pressure transducer location) is defined by the excellent correlation between the experimental results and the results computed using convolution. If predicted results do not compare well with measured results, this could be an indication that some nonlinearity has influenced the measured response.

In addition, because deconvolution involves input/output correlation, any uncorrelated white noise (measurement noise) is easily filtered out. Simple low-pass or high-pass filters would not be able to match this level of filtering capability and much more sophisticated band-pass filters would have to be introduced. However, even with band-

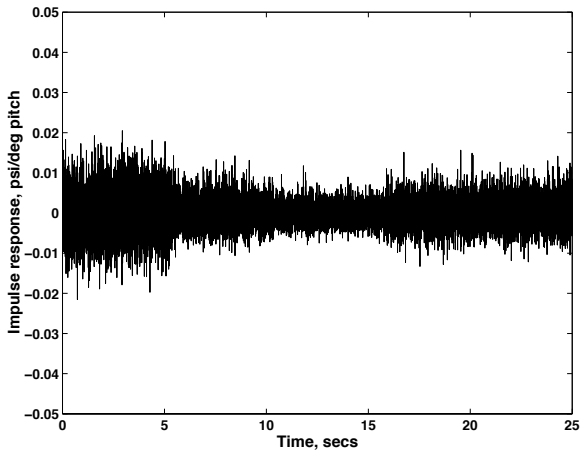

a) Time domain

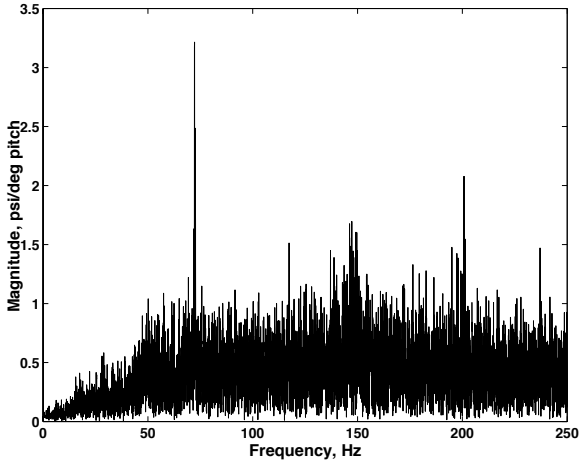

b) Frequency domain

Fig. 16 Pressure impulse response obtained via deconvolution for the RSM; time domain and frequency domain (magnitude).

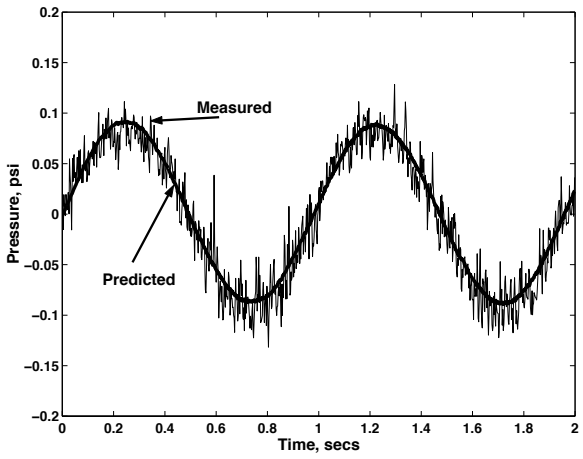

a) Time domain

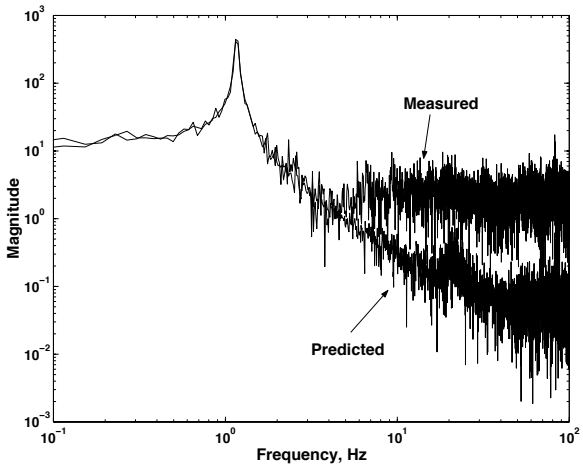

b) Frequency domain

Fig. 17 Measured and predicted pressure responses due to a 1.2 Hz sinusoidal motion of the OTT for the RSM; time domain and frequency domain (magnitude).

pass filters, the question of which frequency range to filter would remain a serious question for the analyst. Deconvolution automatically handles the filtering without a priori definition of a frequency range where filtering is desired. Analysis of these results can subsequently be used to identify regions of linear and nonlinear behavior which will be helpful in understanding dominant flow physics.

Benchmark Supercritical Wing

For the BSCW on the OTT, results are presented for pressure measurements at the trailing edge, at a Mach number of 0.5, a dynamic pressure of 100 psf, and zero degrees angle of attack.

Figure 19 presents the measured and predicted pressure responses due to a 2 Hz sinusoidal motion of the OTT in the time domain and frequency domain (magnitude). The comparison is very good with excellent filtering of the uncorrelated noise.

Finally, Figure 20 presents the measured and predicted pressure responses due to a 15 Hz sinusoidal motion of the OTT in the time domain and frequency domain (magnitude). For this case the comparison is good but Figure 20(a) indicates a difference in the response between the upper and lower portions of the measured response not captured by the predicted response. Additional analyses are required to determine if this difference is due to a possible nonlinear effect. Although at this subsonic Mach number nonlinear aerodynamic effects are not expected in general, since this pressure measurement is at the trailing edge, some local flow separation induced by the higher frequency may be occuring.

Concluding Remarks

The identification of computational and experimental reduced-order models (ROMs) for unsteady aerodynamic and aeroelastic analyses was presented. Results included the implementation of the ROM technique into the CFL3Dv6.0 code, creation of a state-space model of the unsteady aerodynamic system using CFD-based responses, and

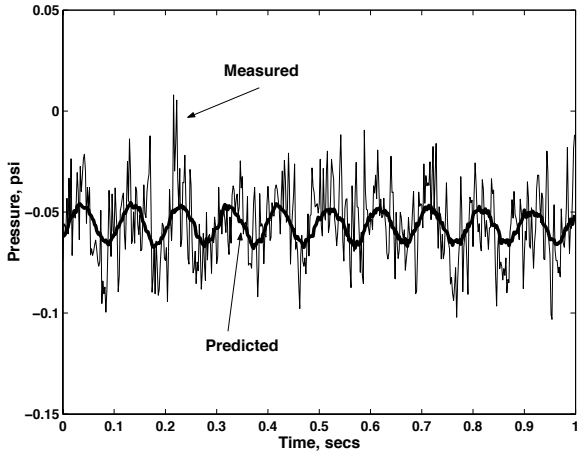

a) Time domain

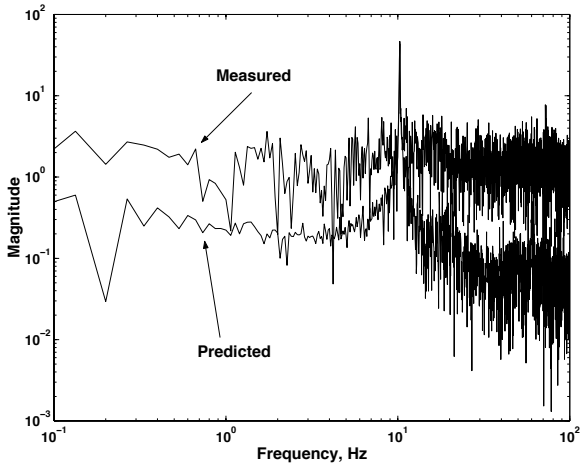

b) Frequency domain

Fig. 18 Measured and predicted pressure responses due to a 10.1 Hz sinusoidal motion of the OTT; time domain and frequency domain (magnitude).

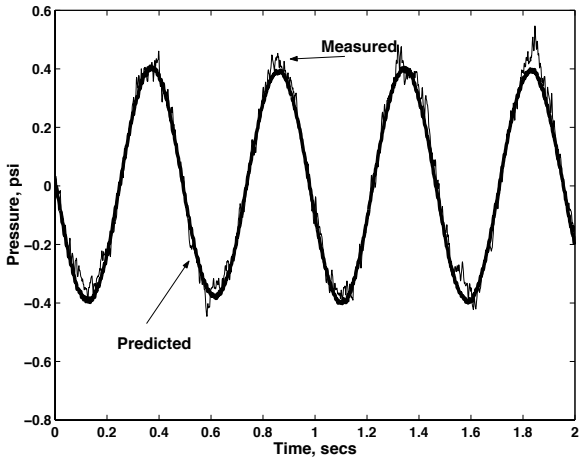

a) Time domain

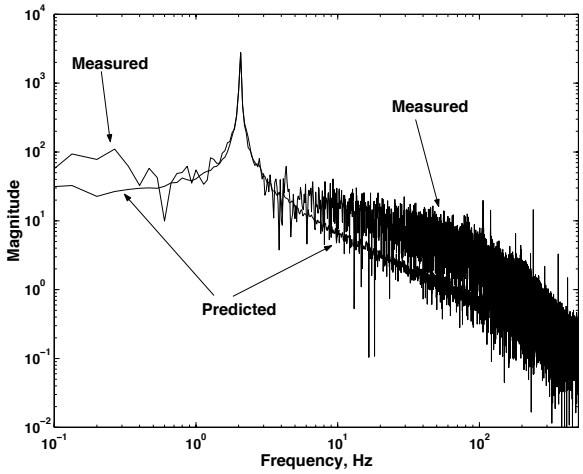

b) Frequency domain

Fig. 19 Measured and predicted pressure responses due to a 2 Hz sinusoidal motion of the OTT for the BSCW; time domain and frequency domain (magnitude).

integration of the state-space ROM into an aeroelastic simulation using the MATLAB/SIMULINK environment. The results presented for the identification of an experimental ROM included results for two wind-tunnel models: a Rigid Semispan Model (RSM) and a supercritical rectangular wing (BSCW). The experimental ROM identification method was described and used to predict the pressure responses due to various sinusoidal oscillations of the Oscillating Turntable (OTT) at NASA Langley's Transonic Dynamics Tunnel (TDT). The accuracy of the method was evaluated and the results presented can be used to gain insight regarding the dominant unsteady flow physics. In addition, potential use of the method for data filtering applications was described.

References

[1]Beran, P. S. and Silva, W. A., "Reduced-Order Modeling: New Approaches for Computational Physics," *Presented at the 39th AIAA Aerospace Sciences Meeting, 8-11 January 2001, Reno,NV*, January 2001.

[2]Silva, W. A., Beran, P. S., Cesnik, C. E. S., Guendel, R. E., Kurdila, A., Prazenica, R. J., Librescu, L., Marzocca, P., and Raveh, D., "Reduced-Order Modeling: Cooperative Research and Development at the NASA Langley Research Center," *CEAS/AIAA/ICASE/NASA International Forum on Aeroelasticity and Structural Dynamics*, June 2001.

[3]Silva, W. A., "Reduced-Order Models Based on Linear and Nonlinear Aerodynamic Impulse Responses," *CEAS/AIAA/ICASE/NASA International Forum on Aeroelasticity and Structural Dynamics*, June 1999.

[4]Silva, W. A., *Discrete-Time Linear and Nonlinear Aerodynamic Impulse Responses for Efficient CFD Analyses*, Ph.D. thesis, College of William & Mary, December 1997.

[5]Silva, W. A., "Application of Nonlinear Systems Theory to Transonic Unsteady Aerodynamic Responses," *Journal of Aircraft*, Vol. 30, 1993, pp. 660–668.

[6]Raveh, D. E., Levy, Y., and Karpel, M., "Aircraft Aeroelastic Analysis and Design Using CFD-Based Unsteady Loads," *41st Structures, Structural Dynamics, and Materials Conference*, No. 2000-1325, Atlanta, GA, April 2000.

[7]Hong, M. S., Kuruvila, G., Bhatia, K. G., SenGupta, G., and Kim, T., "Evaluation of CFL3D for Unsteady

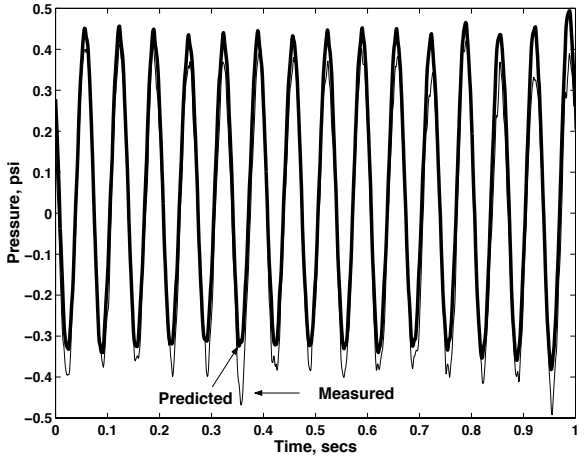

a) Time domain

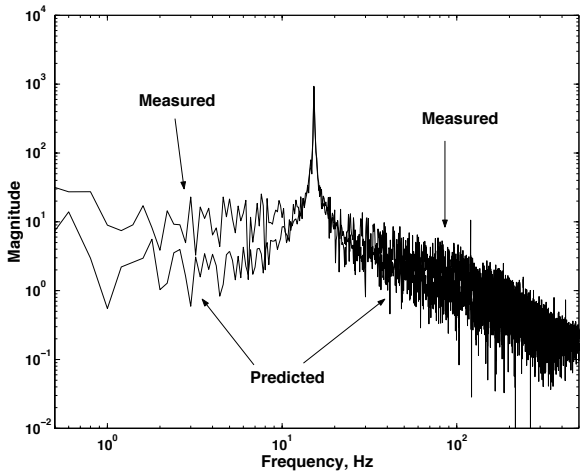

b) Frequency domain

Fig. 20 Measured and predicted pressure responses due to a 15 Hz sinusoidal motion of the OTT for the BSCW; time domain and frequency domain (magnitude).

Pressure and Flutter Predictions," *Proceedings of the 44th Structures, Structural Dynamics and Materials Conference*, No. 03-1923, Norfolk, VA, April 2003.

[8]Dowell, E. H. and Hall, K. C., "Modeling of Fluid-Structure Interaction," *Journal of Annual Review of Fluid Mechanics*, Vol. 33, 2001, pp. 445–490.

[9]Lucia, D. J., Beran, P. S., and Silva, W. A., "Aeroelastic System Development Using Proper Orthogonal Decomposition and Volterra Theory," *Proceedings of the 44th Structures, Structural Dynamics and Materials Conference*, No. 03-1922, Norfolk, VA, April 2003.

[10]Dowell, E. H., Hall, K. C., and Romanowski, M. C., "Eigenmode Analysis in Unsteady Aerodynamics: Reduced Order Models," *Applied Mechanical Review*, Vol. 50, No. 6, June 1997, pp. 371–385.

[11]Baker, M. L., *Model Reduction of Large, Sparse, Discrete Time Systems with Application to Unsteady Aerodynamics*, Ph.D. thesis, University of California at Los Angeles, 1996.

[12]Seidel, D. A., Bennett, R. M., and Ricketts, R. H., "Some Recent Applications of XTRAN3S," AIAA Paper 83-1811.

[13]Lee-Rausch, E. M. and Batina, J. T., "Wing Flutter Computations Using an Aerodynamic Model Based on the Navier-Stokes Equations," *Journal of Aircraft*, Vol. 33, 1993, pp. 1139–1148.

[14]Raveh, D., Levy, Y., and Karpel, M., "Aircraft Aeroelastic Analysis and Design Using CFD-Based Unsteady Loads," AIAA Paper 2000-1325, April 2000.

[15]Raveh, D. and Mavris, D., "Reduced-Order Models Based on CFD Impulse and Step Responses," *Proceedings of the 42nd AIAA/ASME/ASCE/AHS/ASC Structures, Structural Dynamics, and Materials Conference and Exhibit*, No. 2001-1527, Seattle, WA, April 2001, AIAA-01-1527.

[16]Guendel, R. E. and Cesnik, C. E. S., "Aerodynamic Impulse Response of a Panel Method," AIAA Paper No. 2001-1210, to be presented at the 42nd Structures, Structural Dynamics, and Materials Conference, Seattle, WA.

[17]Roger, K. L., "Airplane Math Modeling Methods for Active Control Design," Agard-cp-228, Aug. 1977.

[18]Karpel, M., "Time Domain Aeroservoelastic Modeling Using Weighted Unsteady Aerodynamic Forces," *Journal of Guidance, Control, and Dynamics*, Vol. 13, No. 1, 1990, pp. 30–37.

[19]Gupta, K. K., Voelker, L. S., Bach, C., Doyle, T., and Hahn, E., "CFD-Based Aeroelastic Analysis of the X-43 Hypersonic Flight Vehicle," *Proceedings of the 39th Aerospace Sciences Meeting and Exhibit*, No. 2001-0712, Reno, CA, Jan. 2001.

[20]Cowan, T. J., Jr., A. S. A., and Gupta, K. K., "Accelerating CFD-Based Aeroelastic Predictions Using System Identification," *36th AIAA Atmospheric Flight Mechanics Conference and Exhibit*, No. 2001-0712, Boston, MA, Aug. 1998, pp. 85–93, AIAA-98-4152.

[21]Cowan, T. J., Jr., A. S. A., and Gupta, K. K., "Development of Discrete-Time Aerodynamic Model for CFD-Based Aeroelastic Analysis," *Proceedings of the 37th Aerospace Sciences Meeting and Exhibit*, No. 1999-0765, Reno, CA, Jan. 1999, AIAA-99-0765.

[22]Rodrigues, E. A., "Linear/Nonlinear Behavior of the Typical Section Immersed in Subsonic Flow," *Proceedings of the 42nd AIAA/ASME/ASCE/AHS/ASC Structures, Structural Dynamics, and Materials Conference and Exhibit*, No. 2001-1584, Seattle, WA, April 2001, AIAA-01-1584.

[23]Silva, W. A. and Bartels, R. E., "Development of Reduced-Order Models for Aeroelastic Analysis and Flutter Prediction Using the CFL3Dv6.0 Code," *Proceedings of the 43rd Structures, Structural Dynamics and Materials Conference*, No. 02-1596, Denver, CO, April 2002.

[24]Silva, W. A., Keller, D. F., Florance, J. R., Cole, S. R., and Scott, R. C., "Experimental Steady and Unsteady Aerodynamic and Flutter Results for HSCT Semispan Models," *AIAA/ASME/ASCE/AHS/ASC 41st Structures, Structural Dynamics, and Materials Conference*, No. 2000-1697, April 2000.

[25]Piatak, D. J. and Cleckner, C. S., "A New Forced Oscillation Capability for the Transonic Dynamics Tunnel," *40th Aerospace Sciences Meeting and Exhibit*, Reno, NV, Jan. 2002.

[26]Murphy, P. C. and Klein, V., "Estimation of Aircraft Unsteady Aerodynamic Parameters from Dynamic Wind Tunnel Testing," *AIAA Atmospheric Flight Mechanics Conference and Exhibit*, No. 01-2975, Montreal, Canada, Aug. 2001.

[27]Scott, R. C., Silva, W. A., Keller, D. F., and Florance, J. R., "Measurement of Unsteady Pressure Data on a Large HSCT Semispan Wing and Comparison with Analysis," *Proceedings of the 43rd AIAA/ASME/ASCE/AHS/ASC Structures, Structural Dynamics, and Materials Conference*, No. 02-1648, Denver, CO, April 2002.

[28]Parekh, D. E. and Glezer, A., "AVIA: Adaptive Virtual Aerosurface," *Fluids 2000 Conference and Exhibit*, No. 00-2474, Denver, CO, June 2000.

[29]Honohan, A. M., Amitay, M., and Glezer, A., "AVIA: Adaptive Virtual Aerosurface," *Fluids 2000 Conference and Exhibit*, No. 00-2401, Denver, CO, June 2000.

[30]Chatlynne, E., Rumigny, N., Amitay, M., and Glezer, A., "Virtual Aero-Shaping of a Clark-Y Airfoil Using Synthetic Jet Actuators," *39th Aerospace Sciences Meeting and Exhibit*, No. 01-0732, Reno, NV, Jan. 2001.

[31]Amitay, M., Horvath, M., Michaux, M., and Glezer, A., "Virtual Aerodynamic Shape Modification at Low Angles of Attack using Synthetic Jet Actuators," *31st AIAA Fluid Dynamics Conference and Exhibit*, No. 01-2975, Anaheim, CA, June 2001.

[32]Juang, J.-N. and Pappa, R. S., "An Eigensystem Realization Algorithm for Modal Parameter Identification and Model Reduction," *Journal of Guidance, Control, and Dynamics*, Vol. 8, 1985, pp. 620–627.

[33]"Registered Product of the MathWorks, Inc." .

[34]Silva, W. A., Piatak, D. J., and Scott, R. C., "Identification of Experimental Unsteady Aerodynamic Impulse Responses," *Proceedings of the 44th Structures, Structural Dynamics and Materials Conference*, No. 03-1959, Norfolk, VA, April 2003.

[35]Krist, S. L., Biedron, R. T., and Rumsey, C. L., "CFL3D User's Manual Version 5.0," Nasa langley research center, 1997.

[36]Bartels, R. E., "Mesh Strategies for Accurate Computations of Unsteady Spoiler and Aeroelastic Problems," *AIAA Journal of Aircraft*, Vol. 37, 2000, pp. 521–525.

[37]Roe, P. L., "Approximate Riemann Solvers, Parameter Vectors, and Difference Schemes," *Journal of Computational Physics*, Vol. 43, 1981, pp. 357–372.

[38]Juang, J.-N., Phan, M., Horta, L. G., and Longman, R. W., "Identification of Observer/Kalman Filter Markov Parameters: Theory and Experiments," *Journal of Guidance, Control, and Dynamics*, Vol. 16, 1993, pp. 320–329.

[39]Juang, J.-N., *Applied System Identification*, Prentice-Hall PTR, 1994.

[40]Corliss, J. M. and Cole, S. R., "Heavy Gas Conversion of the NASA Langley Transonic Dynamics Tunnel," *Proceedings of the 20th Advanced Measurements and Ground Testing Technology Conference*, No. 98-2710, Albuquerque, NM, June 1998.

[41]Cole, S. R. and Rivera Jr, J. A., "The New Heavy Gas Testing Capability in the NASA Langley Transonic Dynamics Tunnel," *Royal Aeronautical Society Wind Tunnels and Wind Tunnel Test Techniques Forum*, No. No. 4, Cambridge, UK, April 1997.

[42]Bennett, R. M., Eckstrom, C. V., Rivera, J. A., Dansberry, B. E., Farmer, M. G., and Durham, M. H., "The Benchmark Aeroelastic Models Program-Description and Highlights of Initial Results," *NASA TM-104180*, Dec. 1991.

[43]Dansberry, B. E., Durham, M. H., Bennett, R. M., Rivera, J. A., Silva, W. A., and Wieseman, C. D., "Experimental Unsteady Pressures at Flutter on the Supercritical Wing Benchmark Model," *AIAA/ASME/ASCE/AHS/ASC 34th Structures, Structural Dynamics, and Materials Conference*, La Jolla, CA, April 1993.

[44]Hajj, M. R. and Silva, W. A., "Nonlinear Flutter Aspects of the Flexible HSCT Semispan Model," *Proceedings of the 44th Structures, Structural Dynamics and Materials Conference*, No. 2003-1515, Norfolk, VA, April 2003.

[45]Gordnier, R. E. and Melville, R. B., "Transonic Flutter Simulations Using an Implicit Aeroelastic Solver," *AIAA Journal of Aircraft*, Vol. 37, 2000, pp. 872–879.

[46]E. C. Yates, J., Land, N. S., and J. T. Foughner, J., "Measured and Calculated Subsonic and Transonic Flutter Characteristics of a 45-degree Swept-Back Wing Planform in Air and in Freon-12 in the Langley Transonic Dynamics Tunnel," Tech. rep., NASA, TN D-1616, 1963.